The influence of the global atmospheric properties on the detection of UHECR by EUSO on board of the ISS

C. Bérat, D. Lebrun, A. Stutz

The Influence of the Global Atmospheric Properties on the detection of UHECR by EUSO on board of the ISS

Corinne BERAT, Didier LEBRUN, Anne STUTZ
ISN- Grenoble

The *Extreme Universe Space Observatory* (EUSO) project is aimed to detect from space the Extensive Air Showers (EAS) produced by Ultra High Energy Cosmic Rays (UHECR) when entering the Earth's atmosphere, by the use of a telescope located on the International Space Station. The secondary particles in the shower produce fluorescence and Cherenkov light by interacting with the air molecules. The Earth's atmosphere being the detection medium, it is mandatory to know its characteristics at the place and time an EAS develops.

Here we report on various aspects of basic atmospheric properties which can have a noticeable influence on the light production in the EAS and the light transport to the detector. By basic properties we mean pressure, temperature and composition as a function of altitude, geographical location and date. Since the EUSO telescope will be installed on the ISS, which has a revolution time of 92 minutes on an orbit inclined by 51.6 degrees, these global characteristics of atmosphere in the field of view of EUSO will change minute by minute.

The aim of this note is to present some aspects of atmospheric parameters relevant for EUSO Their variability with time and location and the consequences on the detection are emphasized. In the first part, several atmospheric models and databases, which can be used in order to prepare the EUSO mission, are presented. In the second part, the variations of nitrogen number densities and the subsequent variations of the fluorescence yield is illustrated. In the third part, the influence of the atmospheric conditions variations on the identification of the primary cosmic ray is pointed out. Finally, the airglow variation and its impact on the night sky background are studied.

1- Atmospheric Models

The US Standard Atmosphere 1976 models [1] are commonly used in the atmosphere community. Based on rocket and satellite data and perfect gas theory, the atmospheric densities and temperatures are represented from sea level to 1000 km. Below 32 km the U.S. Standard Atmosphere is identical with the Standard Atmosphere of the International Civil Aviation Organization (ICAO). The U.S. Standard Atmospheres 1976 consist of single profiles representing the idealized, steady-state atmosphere for moderate solar activity. Parameters listed include temperature, pressure, density, acceleration caused by gravity, pressure scale height, number density, mean particle speed, mean collision frequency, mean free path, mean molecular weight, sound speed, dynamic viscosity, kinematical viscosity, thermal conductivity, and geo-potential altitude. The altitude resolution varies from 0.05 km at low altitudes to 5 km at high altitudes. The U.S. Standard Atmosphere Supplements, includes tables of temperature, pressure, density, sound speed, viscosity, and thermal conductivity for five northern latitudes (15, 30, 45, 60, 75), for summer and winter conditions.

The grid in latitude, longitude and time may be not precise enough for our purpose. Using US standard values as inputs whatever the space-time location of the shower can lead to large systematic errors, in the CR energy determination or particle identification.

As far as we are concerned by the global properties and profiles such as pressure, temperature and the number densities of the main constituents it seems better to use the empirical models recommended by the Committee for Space Research (COSPAR). These models are implemented with recent data and are based on the COSPAR International Reference Atmosphere CIRA-86, merged with the Mass-Spectrometer-Incoherent- Scatter (MSIS) model for the upper part of atmosphere. The last available version NRLMISE-00 Model 2001 [2] was used here. The increment of the model concerns particularly the lower atmosphere part, CIRA was implemented with averages from the National Meteorological Center. These empirical atmosphere models provide the profiles of the main constituents and properties (including solar atmospheric data) from ground to 1000 km; it is based on 40 years of data of various types and is continuously updated. It can be used in various fields of EUSO simulation from fluorescence yield variation through nitrogen number density, to airglow through atomic oxygen profile, even on the mechanical side evaluating the impinging of atomic species at 400 km on various part of the telescope. Neutral densities from ground to thermosphere are given within in a latitude, longitude and date grid, which can be easily accommodated to the EUSO trajectory purpose. Forty years fluctuations at a given location can be extracted day by day or hour by hour at a given altitude…and so on.

The MSISE model doesn't contain secondary constituents at low concentration at a given altitude such as water vapor, ozone or aerosols, which are of importance for light production and transmission. This lack of information can be recovered by the use of US-Standard Atmosphere 1976 profiles or by the data of a dedicated measurement.

In the next picture is presented a comparison between US-Standard and NRLMSISE density profiles from ground to 20 km, in order to check that using the data from NRLMSISE, the profiles of the US standard models can be reproduced. Five among usual profiles are shown: Mid Latitude Summer and Winter, Sub-arctic Summer and Winter and Tropical. They are compared here with mean values obtained from NRLMISE00 in almost the same conditions. However some parameters were not averaged. We performed a longitude average, but not a monthly average neither a local solar time average while day to night variations are expected. Nevertheless, even with this lack of precision in the comparison, one sees that both profiles are consistent within ±2.5% at all altitudes.

In order to compare, the inset figure shows the expected variation between US-Mid Latitude Summer and US-Standard Atmosphere.

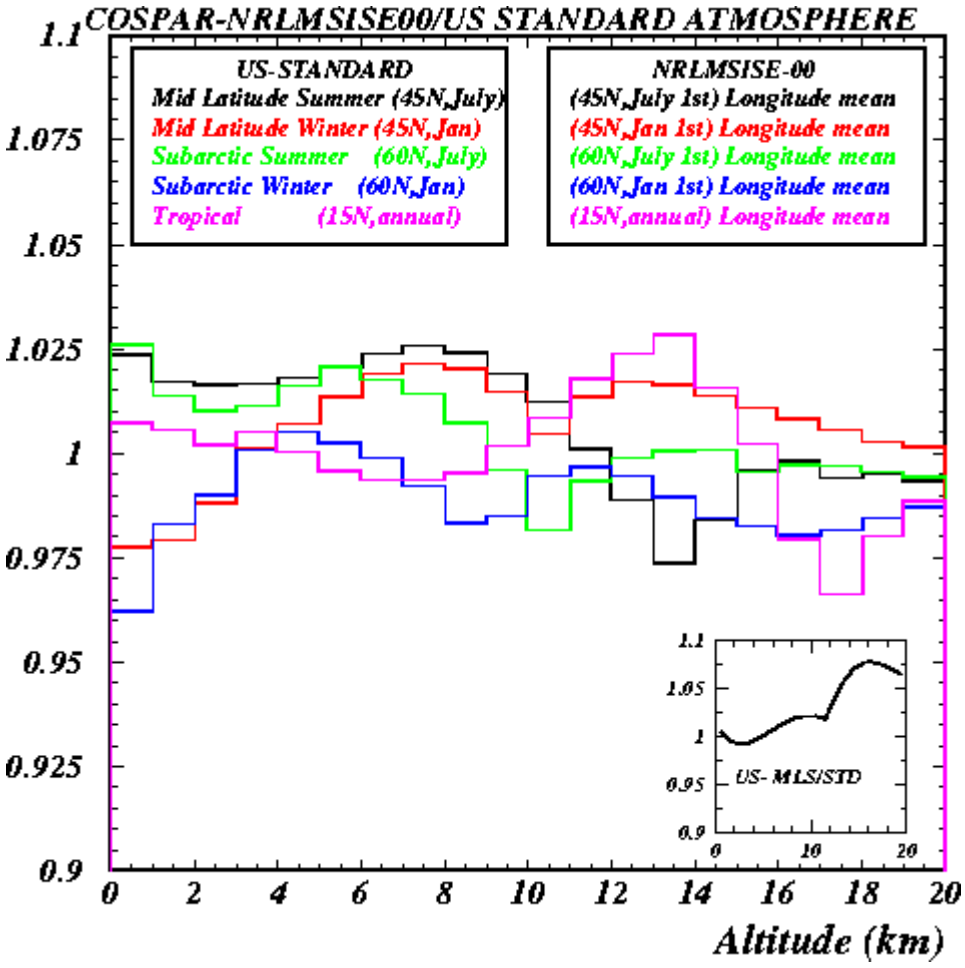

Figure 1: Ratio of density profile obtained from US standard model on one hand and NRLMSISE data at the same latitude and at a similar date on the other hand, as a function of the altitude.

2-Nitrogen number density and Fluorescence Yield

Among the most determinant parameters are the number densities of the most abundant species entering the composition of atmosphere: they dominate the fluorescence yield and the molecular scattering, which is the most important process in the radiative transfer.

For the present studies, the MSIS-E-90 model, which is continuously updated since 1960, is used. As mentioned in the first section, it gives the number densities of various species as a function of altitude, latitude, longitude, time in the year, time in the day (day or night). Fluctuations at a given place or time can be evaluated from 40 years data. For example the N_2 number density, which is an important quantity governing the fluorescence yield since it is roughly proportional to, is shown in Figure 2.

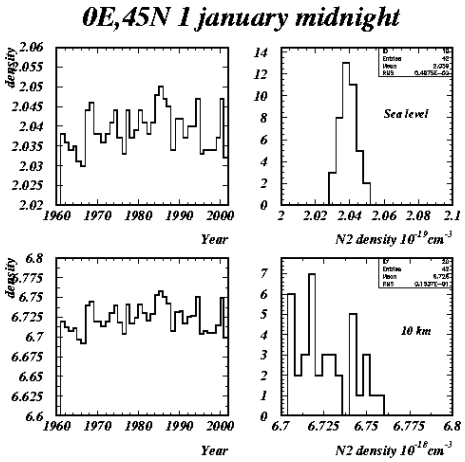

Fig. 2: Nitrogen density over years at sea level and at an altitude of 10 km.

A second aspect of global properties is linked also to the trajectory of the station. The N_2 density at ground level around earth and at a given date is drawn on Figure 3 (the profile with altitude shows similar shape).One observes clearly the latitude variations from low densities near equator to higher density to the poles, here higher in northern hemisphere due to the winter date selection. One also observes a longitude modulation due to local time variation with respect to the sun. Superimposed is shown one possible trajectory of the station revealing the ~10% variation of the density along the track in a very short time

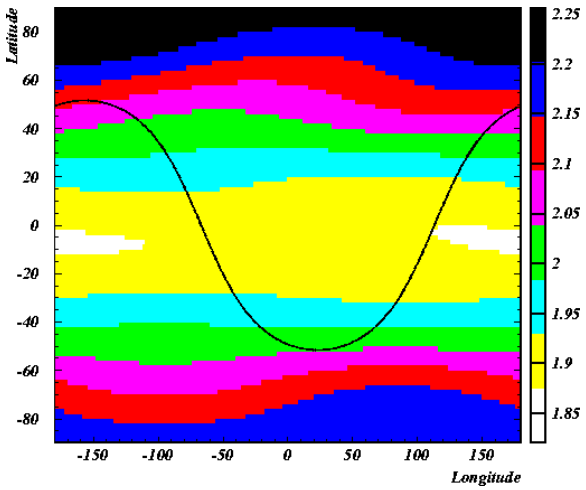

Figure3: Nitrogen density, at a given date: the density at ground level depends on latitude and longitude. One ISS trajectory is shown (black curve).

During one day, the ISS, whose rotation period is 92 minutes, makes fifteen rotations around the globe. Along the trajectory the number density of the observed atmosphere varies, and then the fluorescence yield varies too. In Figure 4, the variation of the N2 density at sea level

is shown versus time corresponding to the ISS trajectory. Along with the path of ISS around the earth (upper-left), the molecular nitrogen density varies according to the location exhibiting an oscillating behaviour (upper-right); the maxima are for northern latitudes (in winter in this case), the smaller maxima for southern locations. The minima are for equatorial latitudes. One observes a longitudinal modulation for the maxima, while attenuated for southern locations; equatorial values do not exhibit strong variations with longitude. The amplitude of variations exceeds 10%. However since observations by EUSO will take place only at night, the variations expressed as a function of the local solar time(LST) (lower-left) show a smaller amplitude when limited by LST=0 $\pm$ 4. At last the detailed variations for one revolution (92 minutes) as a function of time (lower-right) reveals the rapid variation with a 23 minutes period corresponding to ¼ of a revolution.

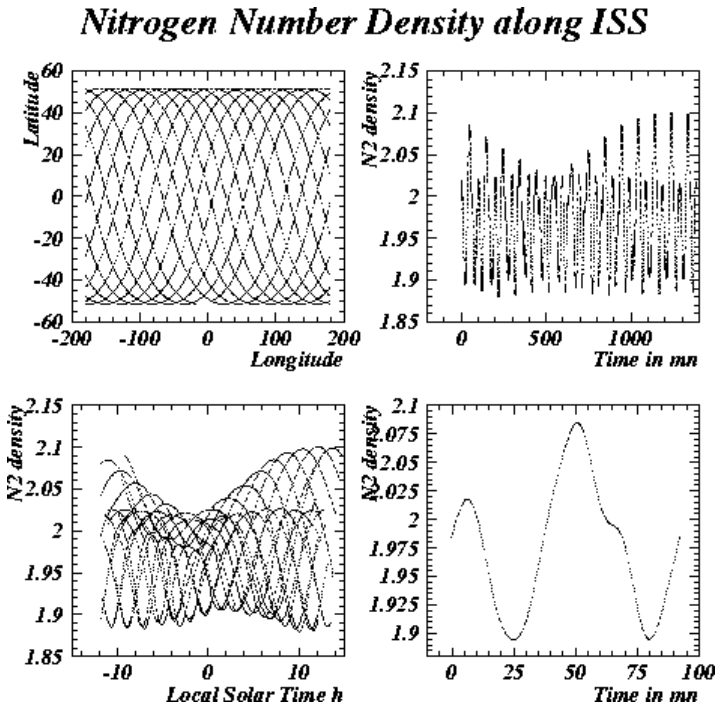

Figure 4: Variation of the N_2 density (at sea level) versus time corresponding to the ISS trajectory

Upper-Left : Projection at ground of the 15 revolutions of ISS during one day
Upper-Right: N_2 density variation with time (along trajectory) during one day
Lower Left : N_2 density variation with Local Solar Time for the 15 revolutions
Lower-Right: N_2 density variation with time for one revolution

A complete calculation linking the fluorescence yield to the nitrogen density is in progress but not yet available. In order to give an idea of the influence of such variations on fluorescence yield, calculations are presented in figure 5 for only 3 locations corresponding to a maximum (south and north) and to a minimum (equator). The variations with altitude of the photon yield observed by EUSO for the 3 locations are presented.

Dry atmospheres were used in order not to be confused with water vapour influence on yield. Photon yield was obtained using the complete 2P and 1N fluorescence transitions lines including pressure and temperature dependence and transmitted through the EUSO filters [3]. At this stage the 3 yield curves can be considered as envelopes of the variations with the ISS trajectory.

Cosmic ray showers take place mainly at an altitude below 10 km, where fluorescence exhibits large variations upon location. This must be taken into account in the energy measurement of cosmic rays, and reveals the importance of using a precise atmosphere modelling at the time the shower take place.

One should notice here that the main parameter governing the variation of the yield with altitude is the atmospheric temperature profile, which together with pressure is converted into atmospheric density.

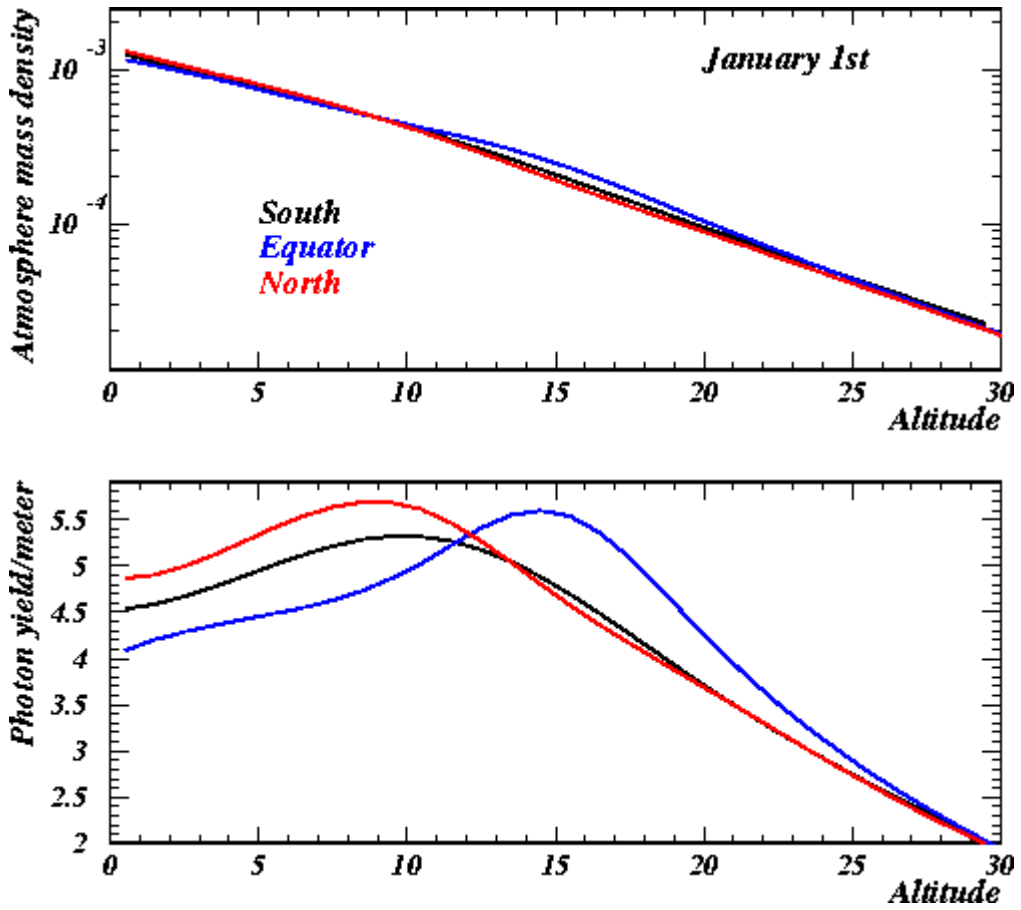

Figure 5:Top: Atmospheric mass density as a function of altitude for North, South and Equatorial latitudes compatible with ISS trajectory. Bottom: Photon yield per meter as a function of altitude for the 3 locations using dry atmospheres and EUSO wavelength bandwidth.

3- Atmospheric mass density and primary cosmic ray identification

Within 23 minutes showers will be detected from Northern latitudes to equator. It is known from ground-based Cosmic Rays detectors that the shower reconstruction is affected by the day by day variations of the atmospheric conditions. This can lead to a misidentification of primary cosmic ray through X_{max} determination: a proton-like shower in winter can simulate a Fe-like shower in summer at a given place, as it has been illustrated by a study performed for the Auger observatory [4]. The same effect is expected to occur within less than 46 minutes which is the mean duration of a EUSO night counting time.

In this section, the influence of the atmospheric condition on the shower development profile is studied. It depends on the nature and energy of the incident particle and on the development of the shower according to the effective atmosphere encountered. At the moment no other effect was added. Light yield profile was fixed for various atmospheres and light transmission coefficient was fixed to 1.

Proton and Fe impinging at 60 degrees were simulated and showers developed at different locations along the trajectory corresponding to one night of ISS flight. In order to simplify we present here shower profiles as a function of altitude for only three realistic locations along ISS as shown on figure 6.

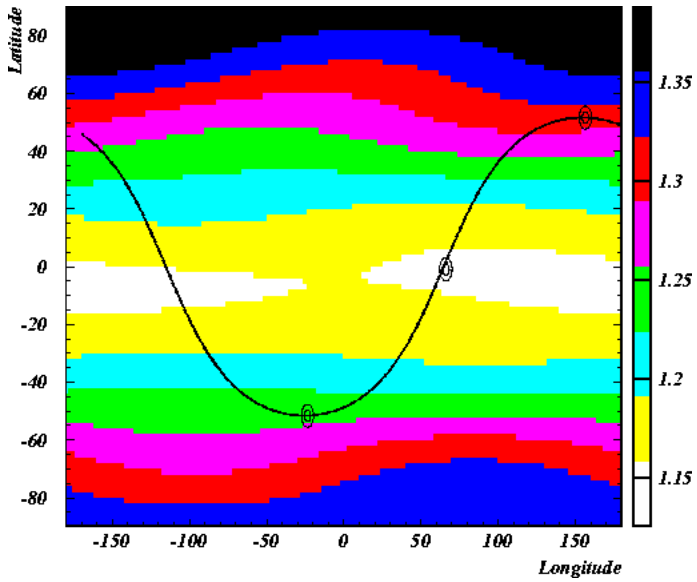

Figure 6: Contour map of atmosphere mass density of atmosphere in mg/cm3 at ground level. One ground projected ISS track is superimposed .The 3 chosen locations are given by latitude, longitude, and time: South :(51.6S,23W) at time=0
Equator: (0.03S,67E) at time=23'
North : (51.6N,150E) at time =46'

Atmospheric profiles of mass density and temperature where obtained from NRLMISE-00 for January 1st at night for the three different locations and injected as input in the Grenoble shower simulation fast code [5]. In the upper-left plot of Figure 7 the mass density profiles of the three atmospheres are presented in comparison with the US–Standard Atmosphere. Differences come from temperature profiles, seasonal variation from south to north, and geo-potential difference at equator whose atmosphere extends higher in altitude.

.

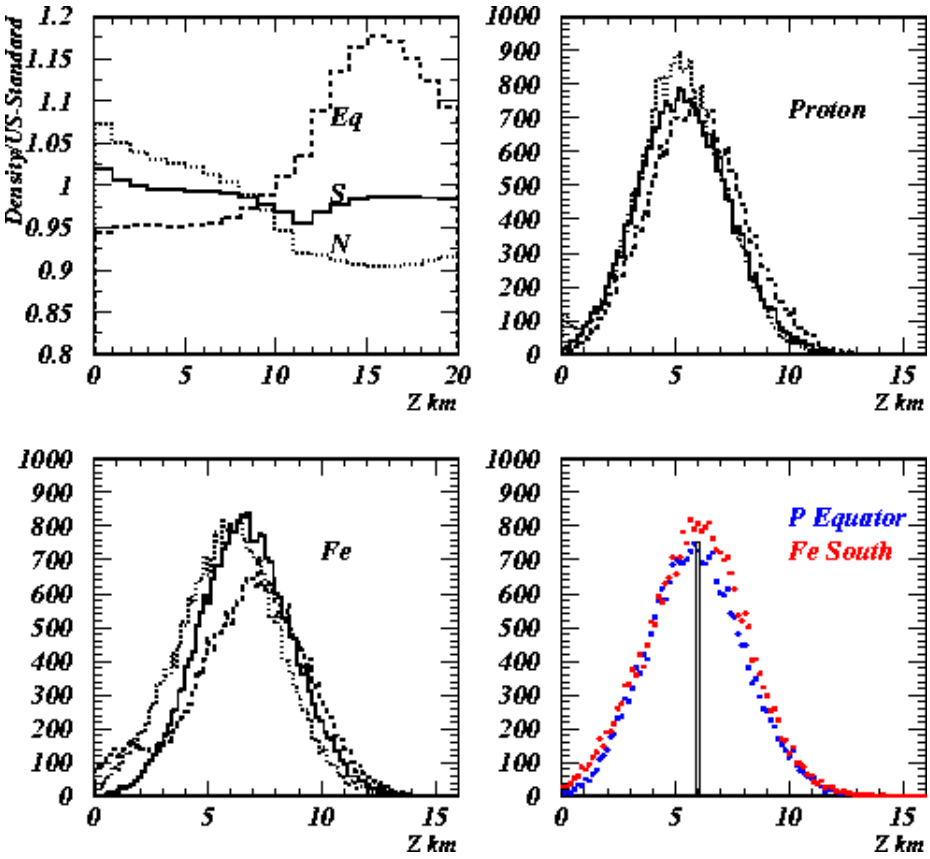

Figure 7: *Cosmic ray showers as a function of altitude*
Upper Left : Mass Density profiles for the 3 locations given above normalized to US-Standard profile
Upper Right : 5.10^{19} Proton shower at 60 degrees at the 3 locations (10 showers added)
Lower Left : 5.10^{19} Fe shower at 60 degrees at the 3 locations
Lower Right : comparison of proton shower at Equator with Fe shower at South Latitude.

For each location a sample of 10 showers initiated by primaries of 5.10^{19} eV at zenith angle of 60 degrees are shown superimposed as a function of the altitude in kilometer; in the upper-right plot of Figure 7, the primaries are protons, and in the lower-left plot, primaries are Iron nuclei. The usual representation of showers as a function of depth in gram/cm^2 is slightly affected by the transformation to altitude which is the real detection frame.
One can see on the lower-right plot on Figure 7 that one can find a solution where proton and Fe are overlapping well, leading to the same value of X_{max} . Since the showers are identical at this stage, no further consideration on light yield production of else will resolve the degeneracy.
The main difference between proton and Fe at the same total energy come from the interaction length which proportional to $(\rho\sigma)^{-1}$; a difference $\Delta\sigma$ can be compensated by an inverse $\Delta\rho$. Proton with lower cross-section than Fe has to cross a denser atmosphere at equator than Fe at south latitude; the probability that the 2 events occur at the same interaction point X_0 and then develop at the same altitude is then increased. Other cases with various energies and impinging shower angles can occur.

4-Airglow variation and night sky background in EUSO

The EUSO telescope on board of the International Space Station will orbit at 400 km and it will point at Nadir for moonless night observation of UHECR air shower fluorescence. The background photon flux will come from the night sky photon flux upward reflected by the earth atmosphere and ground (albedo). This background can be estimated and measured via balloon flights such as in the BABY experiment [6], in similar optical conditions as EUSO, i.e. in the 300 to 400nm bandwidth. Above the sea, BABY observed a flux of 300 to 400 photons/m^2.sr.ns. Among the different components of the night sky background, described for example in reference [7], the most important comes from the so-called Airglow. The upper atmosphere is submitted to an intense flux of solar radiation and cosmic rays. The interaction of these radiations with the oxygen and nitrogen tail profile generates a Chapman layer where the maximum of interactions takes place: ionization, mono-atomic oxygen and nitrogen formation and molecular excitation, those processes generate light emission.

The density of these light sources follows the layer shape, which can be well reproduced by the mono-atomic gas profile obtained via the NRLMSISE-00 model and shown in the figure 8. The mono-atomic Oxygen is concentrated in a thin layer located around 100 km in altitude, while nitrogen layer located around 200 km is wider and extends up to 500 km; both profiles characterize light source profiles.

After the ionization processes, excited molecular gas can be formed via atomic collisions and specific molecular transition radiation then emitted with a delay time constant, allowing emission at night.

While Nitrogen layer location and radiation could be of importance for EUSO background, it will be treated in a further work, and we concentrate here on the Oxygen layer.

In the near UV bandwidth where EUSO will operate, the oxygen layer is of interest. In this layer light emission is due mainly to molecular oxygen Herzberg band transitions, whose strength is concentrated between 300 and 450 nm [7].

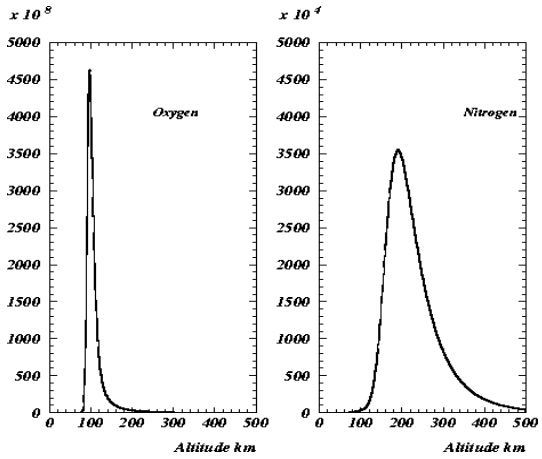

Figure 8: Mono-atomic Oxygen and Nitrogen profiles

The photon flux and spectrum from this layer have been measured and are compiled in reference [7]. The detailed measurement performed at ground at the Calar Alto Observatory and quoted in [7] will be used as a reference. The flux is ~300-400 photons/m^2/sr/ns, depending on the observation conditions, on which we will come back. This is the same order of magnitude as the background measured by BABY looking downward to the ground. This airglow flux, once reflected by a mean earth albedo of 30%, should contribute to at least 100 photons among the 300 photons measured by balloon measurement. The main effect we want to consider here is due to the fact that this airglow source lies at 100 km in altitude. A balloon flight reaching 40 km stays below the airglow and sees it only by reflection on the atmosphere and on the ground, while EUSO located at 400 km and pointing at nadir will see two contributions: one by reflection as the balloon observation does and one in direct view of the airglow. The result will be a background in EUSO of the order of 600 photon/m^2/sr/ns, 2/3 of which comes from the airglow. Since this light emission is the result of the interaction of solar

radiation with high altitude molecular density, a significant variation of its intensity is expected to occur with solar activity, but also with latitude and longitude around the globe.

Due to the variation of exposure time to radiation, day to night and seasonal variations at a given location are also expected. Geomagnetic field affecting the particle spectrum is also important.
The photon flux from airglow is proportional to the mono-atomic oxygen density. This density can be obtained from NRLMSISE-00 model as a function of date time and location. Normalization of the flux was obtained here with the Calar Alto measurement located at (37N, 5W) on June 23rd, 1990 when the solar Index was nearly 180.

A map of the airglow flux can be built from the model computed on that day at night and is shown in figure 9. Having the EUSO trajectory in mind one can easily observe that an amplitude variation by a factor greater than 2 is expected on this particular day.

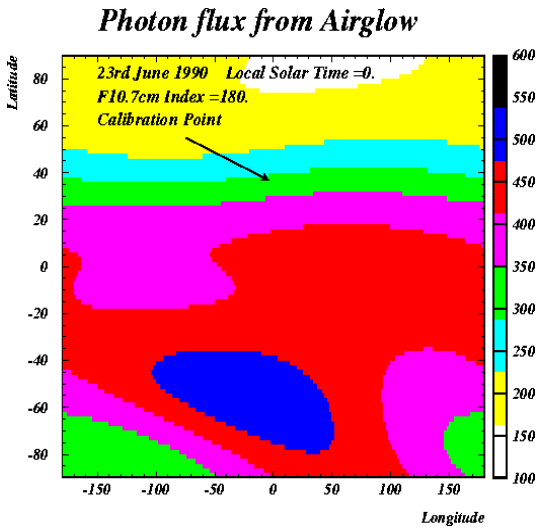

Figure 9: Photon flux from Airglow on June 23rd,1990

Seasonal variations are presented on figure 10 assuming a constant solar flux index. One observes strong variations with time at each location on the earth.

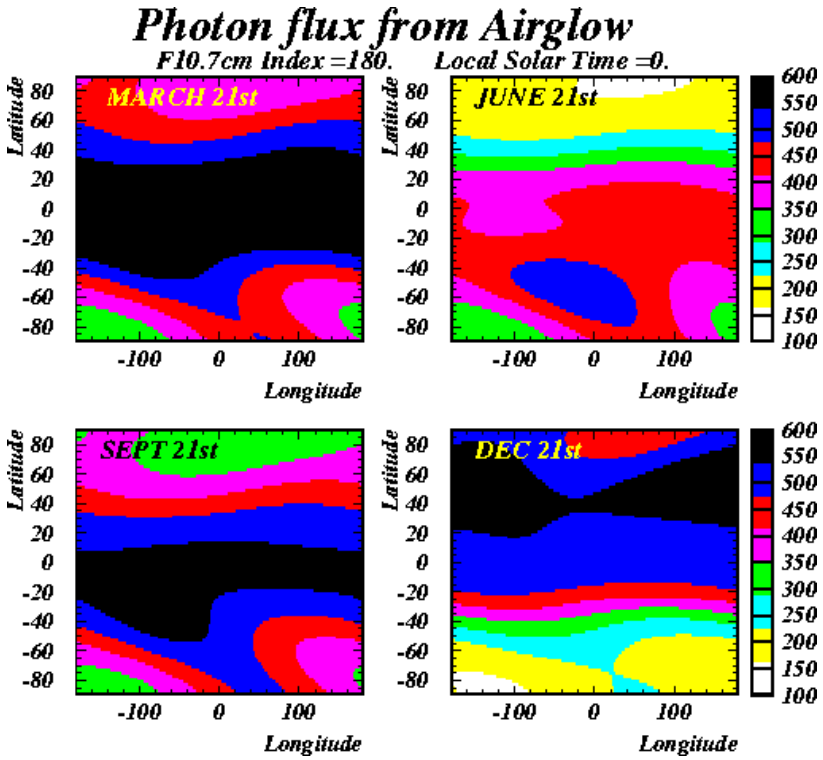

Figure 10: Seasonal variations of airglow flux.

Transformed into the EUSO moving frame the photon flux is presented in figure 11 respective to the ISS trajectory on January 1st (the same as presented on figure 4 for nitrogen densities). The amplitude of variations reach almost a factor of 2 with a high modulation frequency , this justifies to take into account variations on a few minutes time basis. In the particular case of the photon background, the influence on shower detection can be easily deduced mainly linked to the trigger efficiency and threshold detection which could be highly variable along with EUSO track.

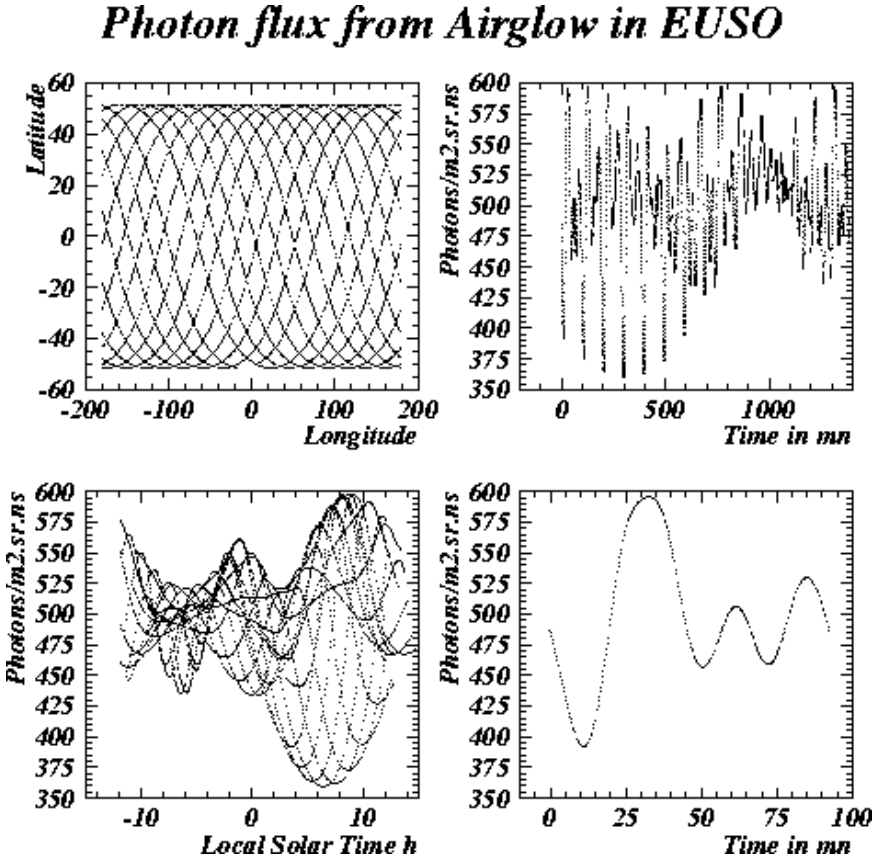

Figure 11*: Variation of the photon flux from airglow versus time corresponding to the ISS trajectory*

Upper-Left : Projection at ground of the 15 revolutions of ISS during one day
Upper-Right: airglow flux variation with time (along trajectory) during one day
Lower-Left : Airglow flux as a function of Local Solar Time for 15 revolutions
Lower-Right: Airglow flux as a function of time for 1 revolution.

1

[1] The solar Index was kept constant at F10.7=180; this value is quiet high and corresponds almost to a maximum of solar cycle. At low solar activities the expected index is around 80 and airglow flux can be reduced by more than 50 %. Variations with solar index are included in the present evaluations but not presented here for simplicity

References

[1] http://nssdc.gsfc.nasa.gov/space/model/atmos/us_standard.html

[2] M.Picone et al. http://nssdc.nasa.gov/space/model/atmos/nrlmsise00.html

[3] D.Lebrun , ISN Grenoble Report-2002-037

[4] B.Keilhauer et al. Auger Technical Note GAP-2002-022

[5] D.Lebrun , ISN Grenoble GEFASS code, unpublished

[6] O. Catalano *et al*., NIM A0(2001)

[7] Ch. Leinert *et al*., Astron. Astrophys. Suppl. Ser. **127**, 1-99 (1998).